Evaluation of Thermal Neutron Scattering Cross Sections for CaH_2

B. K. Laramee, A. I. Hawari

Department of Nuclear Engineering, North Carolina State University, Raleigh, NC 27695, USA
bklarame@ncsu.edu , ayman.hawari@ncsu.edu

INTRODUCTION

Solid metal hydrides have long been considered viable moderators for nuclear reactor designs due to their moderating ratios, hydrogen densities, high dissociation temperatures, and mechanical properties[1]. CaH_2 is an orthorhombic saline-hydride that has recently been investigated and shows promise for use as a moderator in microreactors[2].

At present, there is no Thermal Scatting Law (TSL) evaluation for CaH_2 in the ENDF/B-VIII.0 database. An evaluation does exist in the JEFF-3.3 database[3], performed by Serot[4], however it was limited by the implemented methods and thus both drastically over-predicts the incoherent elastic contribution and completely ignores the coherent elastic contribution to scattering from the metal ions. The thermal neutron scattering cross sections of CaH_2 are evaluated in this work to establish accurate data for use in reactor design. The present evaluation corrects the inaccuracies of the JEFF-3.3 data, and yields three distinct libraries: Ca in CaH_2, H_1 in CaH_2, and H_2 in CaH_2.

THERMAL SCATTERING THEORY

The double-differential scattering cross section, which describes the probability of a neutron of incident energy E scattering to a secondary energy E' through solid angle Ω, is derived from first principles using the First Born Approximation and Fermi's Golden Rule. It is shown in Eq. (1), where k_B is the Botlzmann constant, T is the temperature in Kelvin, $S(\alpha,\beta)$ is the thermal scattering law (TSL, described in the following paragraphs), and σ_{coh} and σ_{inc} are the coherent and incoherent bound nuclear scattering cross sections, respectively.

$$\frac{\partial^2\sigma}{\partial\Omega\partial E'} = \frac{1}{4\pi k_B T}\sqrt{\frac{E'}{E}}\left[\sigma_{coh}S(\alpha,\beta) + \sigma_{inc}S_s(\alpha,\beta)\right] \quad (1)$$

Neutrons exchange energy and momentum with the scattering system according to the TSL, $S(\alpha,\beta)$. This function is a property of the material which describes the probability distribution of energy and momentum states available for the neutron to interact with. It is defined in terms of the dimensionless momentum and energy transfer variables α and β, respectively, and is dependent on temperature. The scattering law can be written in terms of a component that contains inter-atomic interference effects and a component that does not – the distinct-part (S_d) and the self-part (S_s), respectively.

$$S(\alpha,\beta) = S_s(\alpha,\beta) + S_d(\alpha,\beta) \quad (2)$$

The incoherent and Gaussian approximations are invoked in calculating the TSL; the former assumes that the distinct component of the TSL does not contribute to scattering, and thus $S_d = 0$. For crystalline materials, the harmonic approximation allows the TSL to be calculated via a phonon expansion, where the first term corresponds to elastic scattering and all higher-order terms correspond to inelastic scattering via the creation and absorption of phonons (i.e., atomic vibrational quanta). As a result, a crucial step in evaluating the thermal neutron scattering cross sections of a crystal is to calculate its phonon density of states (DOS). This is currently performed via *ab initio* lattice dynamics (AILD) simulations[5,6].

Neutron scattering in hydrogenous materials was investigated by Fermi in the 1930's[7] for a range of incident neutron energies, including thermal energies. While using a much simpler model than present in a modern computational approach, Fermi was able to derive the thermal neutron scattering cross section for a hydrogenous material in terms of the order of magnitude of the bound scattering length of the material. He demonstrated that the scattering cross section shows oscillatory behavior at successive intervals of the ground-state hydrogen energy, which can be easily compared to the results of this paper.

COMPUTATIONAL APPROACH

CaH_2 has an orthorhombic crystal structure belonging to the space group *Pnma*. It has three distinct nonequivalent atom sites, two belonging to hydrogen atoms, notated as H_1 and H_2 in this work, with the other site belonging to the metal ion. The calcium ions form a distorted hexagonal close-packed array[8], while the hydrogen ions are coordinated by calcium tetrahedra and distorted octahedra (for H_1 and H_2, respectively). Figure 1 below shows the crystal structure of the hydride, with the coordination polyhedra for H_1 highlighted.

AILD based on density functional theory (DFT) as implemented in the Vienna *ab initio* simulation package (VASP) using the projector-augmented wave (PAW) method was used to calculate the optimized structure and associated Hellmann-Feynman forces of the CaH_2 crystal[9]. A GGA-PBE

pseudopotential was utilized with a planewave energy cutoff of 675 eV and a 9x9x9 Monkhorst-Pack k-point mesh[10]. The Hellmann-Feynman forces were calculated for an approximately cubic 2x3x1 supercell. These were passed to the PHONON code in order to calculate the phonon dispersion curves and DOS using the dynamical matrix method[11,12].

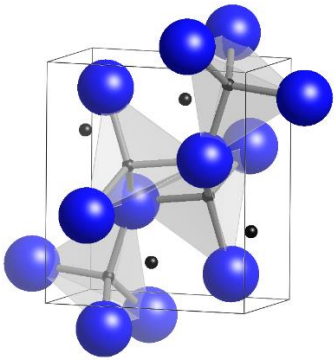

Fig. 1. CaH_2 unit cell with highlighted H_1 coordination polyhedra. The Ca ions are represented by the blue spheres, and the H ions by the smaller black spheres.

After the partial DOS for each nonequivalent atom site were obtained, they were used by the Full Law Analysis Scattering System Hub, *FLASSH*, a code developed by the Low Energy Interaction Physics (LEIP) group at North Carolina State University, to generate the TSLs and subsequent coherent elastic, incoherent elastic, and incoherent inelastic thermal neutron scattering cross sections[13].

RESULTS

The calculated crystal structure parameters and atomic positions show good agreement to experimental values; the former are presented in Table I. Figure 2 compares the calculated total phonon DOS with experiment[14]. The primary peak of the low-energy acoustic mode, corresponding to the vibrations of the heavier metal ion, shows reasonable agreement with experiment. The optical branches, belonging to the hydrogen atoms, also show reasonable agreement, albeit with a slight shift to lower energies.

TABLE I. Calculated Lattice Parameters for CaH_2

Lattice Constant	This Work	Experiment[15]	Error (%)
a (Å)	5.92176	5.92852	0.114
b (Å)	3.57607	3.57774	0.0468
c (Å)	6.78272	6.78956	0.1007

Based on the bound coherent and incoherent scattering cross sections of Ca and H, taken from the NIST database[16] and shown in Table II, the coherent elastic component of the H_1 and H_2, and the incoherent elastic component of the Ca cross section, were neglected. Therefore, the coherent elastic and incoherent inelastic cross sections were calculated for Ca in CaH_2 while the incoherent elastic and incoherent inelastic cross sections were calculated for H_1 and H_2 in CaH_2.

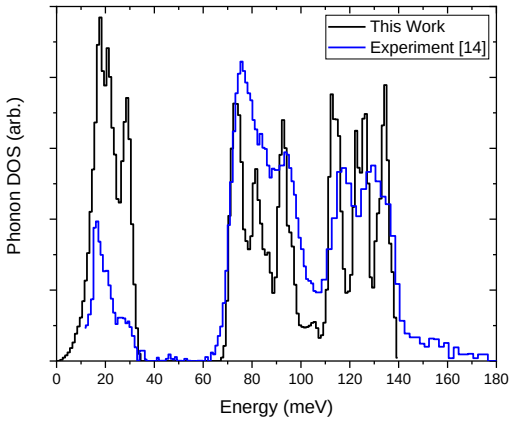

Fig. 2. Phonon DOS for CaH_2 predicted by DFT calculated compared to experimental data.

TABLE II. Coherent and Incoherent Bound Cross Sections

Isotope	σ_b^{coh} [b]	σ_b^{inc} [b]
Ca (natural)	2.64	0.000675
^{1}H	1.7568	80.26

Fig. 3 shows the coherent elastic, inelastic, and total cross sections for Ca in CaH_2 at 296 K. All cross sections were evaluated at the following 8 temperatures: 296, 400, 500, 600, 700, 800, 1000, and 1200 K. The total cross section demonstrates the expected behavior, and asymptotes to the free atom cross section at higher energies. The total cross section for various temperatures is shown in Fig. 4 and is compared to the total cross section for Ca in CaH_2 available in the JEFF-3.3 evaluation. This evaluation neglected coherent elastic scattering and instead used incoherent elastic data that comprised a drastically larger contribution than it should, due to limitations of NJOY[17]. The differences between the two evaluations can clearly be seen in this comparison.

Figure 5 highlights the differences in the total cross sections of the two distinct nonequivalent hydrogen atoms in CaH_2. Note that both display oscillatory behavior at higher energies, as predicted by Fermi[7]. The differences in the cross sections are due to the different partial vibrational DOS of the two atom sites, and the large drop in total cross section beginning around 0.01 eV is due to the relatively large incoherent elastic cross section, which decays exponentially with increasing energy. The total cross sections for H_1 and H_2 in CaH_2 are shown for all evaluated temperatures in Fig. 6 and Fig. 7, respectively.

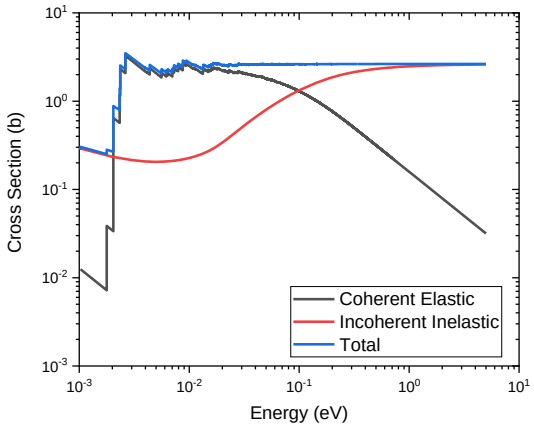

Fig. 3. The coherent elastic, incoherent inelastic, and total scattering cross sections of Ca in CaH_2 at 296 K.

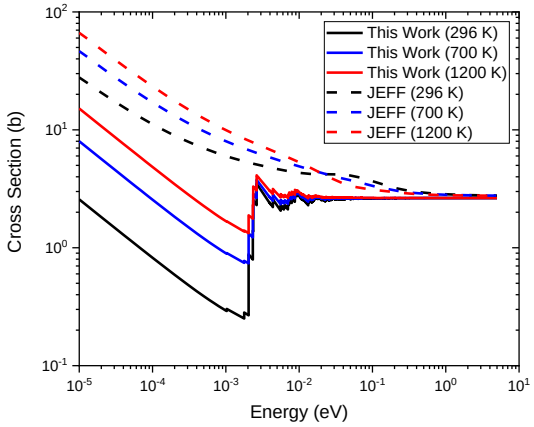

Fig. 4. Total scattering cross sections for Ca in CaH_2 compared to the total cross sections available in the current JEFF-3.3 library for various temperatures.

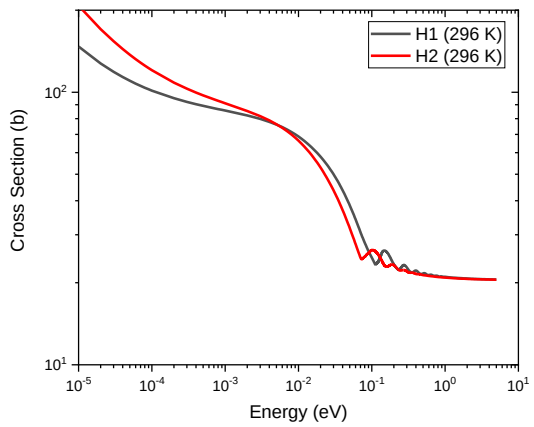

Fig. 5. Total scattering cross sections for H_1 and H_2 in CaH_2 at 296K. The oscillatory behavior of the cross section can be seen beginning around 0.1eV.

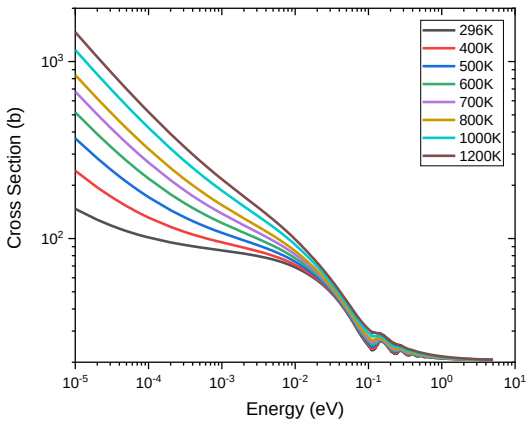

Fig. 6. Total scattering cross sections for H_1 in CaH_2 at various temperatures.

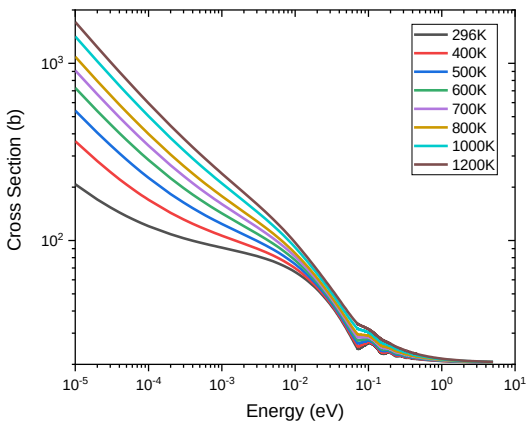

Fig. 7. Total scattering cross section for H_2 in CaH_2 at various temperatures.

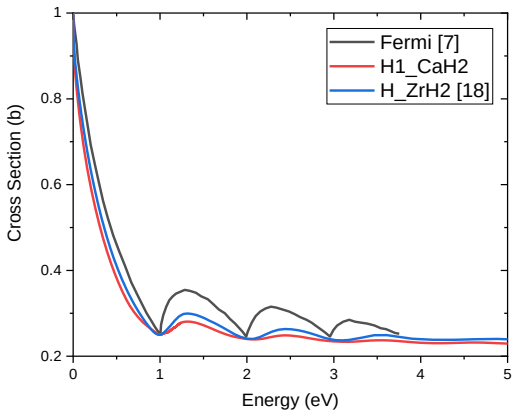

Fig. 8. Comparison between the thermal neutron scattering cross section in a hydrogenous material derived by Fermi and the calculated cross sections for H_1 in CaH_2 at 296 K and H in ZrH_2 at 293.6 K.

As noted in the analysis of the total scattering cross sections for H_1 and H_2, oscillatory behavior is present as the incident neutron energy approaches the ground state hydrogen energy. These results are compared to the results of Fermi's 1936 study in Fig. 8[7]. The plot compares both the cross sections of H_1 in CaH_2 and H in ZrH_2, the latter taken from the ENDF/B-VIII.0 database[18]. The calculated cross sections are normalized such that the energy and cross section of the first oscillatory jump match. Notice that the jumps shown by Fermi closely relate to the actual oscillations of the materials. As mass increases, the curves approach the magnitudes that Fermi showed, for a system where hydrogen is tightly bound by an effectively-infinite mass. The calculated cross sections do not line up exactly with the successive energy intervals shown by Fermi but instead oscillate at higher energies, implying anharmonicity in the real systems as opposed to the perfect harmonic case analyzed by Fermi.

CONCLUSIONS

This work evaluated the thermal neutron scattering cross sections for the three nonequivalent atom sites in CaH_2: Ca, H_1, and H_2. The evaluation for the metal ion is comprised of coherent elastic and inelastic components, while those for the hydrogen ions contain incoherent elastic and inelastic contributions. It has been shown that the new evaluation of Ca in CaH_2 is much more accurate than the existing evaluation in the JEFF-3.3 database. The hydrogen cross sections are kept as two distinct evaluations rather than the averaged evaluation of the existing data, which better captures the individual scattering behavior of each site, especially the higher-energy oscillatory features. No experimental data for the scattering cross sections of CaH_2 is readily available, and thus none is presented for comparison in this work. Future work consists of validation of these results, as well as their submittal to the NNDC for the next ENDF database release.

REFERENCES

[1] W. M MUELLER et al., Metal *Hydrides*. New York: Academic Press, Inc. (1968).

[2] R. KIMURA and S. WADA, "Temperature Reactivity Control of Calcium Hydride–Moderated Small Reactor Core with Poison Nuclides," *Nuclear Science and Engineering*, **193**, *9*, 1013 (2019).

[3] A. J. M. PLOMPEN et al.., "The joint evaluated fission and fusion nuclear data library, JEFF-3.3," *European Physical Journal A*, **56**, *7*, 181 (2020).

[4] O. SEROT, "New results on CaH2 thermal neutron scattering cross sections," *AIP Conference Proceedings*,**769**, *1*, 1446 (2005).

[5] A. I. HAWARI et al., "Ab Initio Generation of Thermal Neutron Scattering Cross Sections," *PHYSOR, The Physics of Fuel Cycles and Advanced Nuclear Systems: Global Developments*, Chicago, IL, 2004.

[6] A. I. HAWARI, "Modern techniques for inelastic thermal neutron scattering analysis," *Nuclear Data Sheets*, **118**, *1*, 172 (2014).

[7] E. FERMI, "On the Motion of Neutrons in Hydrogenous Substances," *Ric. Scientifica*, **2**, 13 (1936).

[8] E. ZINTL and A. HARDER, "Constitution of the Alkaline Earth Hydrides," *Z. Electrochem*, *41*, 33 (1935).

[9] G. KRESSE and D. JOUBERT, "From ultrasoft pseudopotentials to the projector augmented-wave method," *Physical Review B*, **59**, 1785 (1999).

[10] H. J. MONKHORST and J. D. PACK, "Special points for Brillouin-zone integrations," *Physical Review B*, **13**, *12*, 5188 (1976).

[11] K. PARLINSKI, "PHONON," (2013).

[12] K. PARLINSKI et al., "First-Principles Determination of the Soft Mode in Cubic ZrO 2," *Physical Review Letters*, **78**, 4063 (1997).

[13] Y. ZHU and A. I. HAWARI, "Full Law Analysis Scattering System Hub (FLASSH)," *PHYSOR – Reactor Physics Paving the Way for More Efficient Systems,"* Cancun, Mexico (2018).

[14] P. MORRIS et al., "Inelastic neutron scattering study of the vibration frequencies of hydrogen in calcium dihydride," *Journal of Alloys and* Compounds, **363**, *1-2*, 88 (2004).

[15] H. WU et al., "Structure and vibrational spectra of calcium hydride and deuteride," *Journal of Alloys and Compounds*, **436**, *1-2*, 51(2007).

[16] V. F. SEARS, "Neutron scattering lengths and cross sections," *Neutron News*, **3**, *3*, 26 (1992).

[17] D. W. MUIR et al., "The NJOY Nuclear Data Processing System, Version 2016," (2019).

[18] D. A. BROWN et al., "ENDF/B-VIII.0: The 8th Major Release of the Nuclear Reaction Data Library with CIELO-project Cross Sections, New Standards and Thermal Scattering Data," *Nuclear Data Sheets*, **148**, 1 (2018).